



## Improvement of bivalent metal dispersion in ternary layered double oxide (LDO) for efficient anion removal

Yuan Gao<sup>a</sup>, Weikang Shu<sup>a</sup>, Mao Lin<sup>a</sup>, Jia Zhang<sup>a</sup>, Jizhi Zhou<sup>a,\*</sup>, Zhi Ping Xu<sup>b</sup>, Guangren Qian<sup>a</sup>

<sup>a</sup>School of Environmental and Chemical Engineering, Shanghai University, Shanghai 200444, China, Tel. +86-21-66137746; emails: jizhi.zhou@shu.edu.cn (J. Zhou), gaoyuanhong@i.shu.edu.cn (Y. Gao), shuwk@i.shu.edu.cn (W. Shu),

lm0813@yeah.net (M. Lin), irujam@t.shu.edu.cn (J. Zhang), jizhi.zhou@shu.edu.cn (J. Zhou), grqian@shu.edu.cn (G. Qian)

<sup>b</sup>Australian Institution for Biotechnology and Nanomaterial, University of Queensland, Brisbane, Queensland 4072 Australia, Tel. 61-7-33463809; email: gordonxu@uq.edu.au (Z.P. Xu)

Received 1 March 2017; Accepted 17 July 2017

### ABSTRACT

In this study, the removal of tripolyphosphate (TPP) was performed over  $Mg_{2-x}Ca_xFe$  layered double oxide (Fe-LDO,  $x = 0.0-2.0$ ) and  $Mg_{2-x}Ca_xAl$  layered double oxide (Al-LDO,  $x = 0.0-2.0$ ). For the preparation of LDO, the thermal process of the pristine LDHs was carried out by thermal gravity analysis (TGA). It is indicated that the binary metal in  $Mg_{2-x}Ca_xAl$  layered double hydroxide (Al-LDH,  $x = 0.5-1.5$ ) was well dispersed while  $Mg_{2-x}Ca_xFe$ -LDH showed two separated Ca-Fe-LDH and Mg-Fe-LDH phases in the sample. In TPP removal, the removal amount of TPP over  $Mg_2Fe$ -LDO and  $Mg_2Al$ -LDO was 11.8 and 21.4 mg P/g, respectively. In contrast,  $Ca_2Fe$ -LDO and  $Ca_2Al$ -LDO provided 121.0 and 185.0 mg P/g of TPP removal capacity, respectively. Moreover, on ternary  $Mg_{2-x}Ca_xFe$ -LDO and  $Mg_{2-x}Ca_xAl$ -LDO ( $x = 0.5-1.5$ ), the sorption amount of TPP in Al-LDO was higher than that in Fe-LDO. Especially, 117 mg P/g of TPP removal amount was recorded in the case of  $Mg_{0.5}Ca_{1.5}Al$ -LDO. This was attributed to the fact that Al-LDO could be reverted to Mg-Al-LDH framework, which provided OH-metal on the solid surface to improve the TPP adsorption on the adsorbent. The other reason for TPP removal was Ca doping into the Mg-Al-LDH framework in the reformed LDH from LDO, which improved the affinity of TPP to the adsorbent by TPP precipitation. Therefore, our result proposed that it was advisable and feasible to use LDO for the removal of TPP.

**Keywords:** Layered double oxide (LDO); Tripolyphosphate; Precipitation; Adsorption; Ternary metals

### 1. Introduction

Tripolyphosphate (TPP,  $P_3O_{10}^{5-}$ ), as a detergent builder, is widely used in various industrial production and daily life [1,2]. Halliwell et al. [3] found that the concentration of TPP in the inflow reached 2.7 and 1.7 mg/L in peak and in off-peak, respectively, which were more than the prescribed standards (0.5–1.0 mg/L). On the other hand, TPP is one species of condensed phosphates that are formed through an intermediate link ( $PO_3$ ) group linking to the fore-and-aft tetrahedral [ $PO_4$ ]

units [4]. Different from orthophosphate ( $PO_4^{3-}$ ), TPP can be slowly hydrolyzed, because [ $PO_3$ ] link is easily affected by environment and dissociation [5]. Halliwell found that, at 20°C, the half-life of TPP was 3 h in urban sewage. Due to the slow hydrolysis of TPP, those P stored in TPP will gradually release into the water in the form of orthophosphate, which leads to aquatic plants with abundant P, and causes eutrophication [6]. Accordingly, the biological availability of TPP is often overlooked because it cannot be measured by the conventional method of the phosphate detection [7]. With the development of  $^{31}P$  NMR technology, TPP was found to directly promote the growth of plant roots, which resulted in the similar situation to orthophosphate [6]. As a

\* Corresponding author.

result, the presence of TPP is a potential phosphate source that can improve the eutrophication in ecological systems for a long time. Therefore, it is extremely urgent and crucial to develop the technology for the efficient removal of TPP from wastewater.

Removal of TPP includes physicochemical and biological technologies [8]. Among these technologies, the adsorption technique has been recognized as an effective and promising method. Ferrihydrite, aluminum hydroxide, and mesoporous magnesium oxide were used as absorbents [9–12]. Moreover, Ca-abundant animal and plant waste were also used in the adsorption of TPP. For instance, fine grinding of crab shells could remove up to 108.9 mg P/g [13]. Recently, layered double hydroxide (LDH) showed an outstanding capacity for TPP removal (107.8 mg P/g) [14,15]. The removal of triphosphate over LDH mainly underwent the surface adsorption and the near-edge intercalation, which was contributed by the Mg–Al(or Fe)–O structure [14–17].

LDH is a layered material, which is composed of metal ions–formed hydroxide layers with exchangeable anions in the interlayer. The heat treatment of crystalline LDH at higher temperatures (400°C–600°C) leads to the collapse of LDH structure, which changes to amorphous layered double oxide (LDO) [18–20]. The LDH structure could be restored from LDO in the water [21–23]. In this progress, the anion in the water was intercalated into the interlayers, which is called “reformation effect” [24]. This effect can significantly increase its adsorption towards anions. Besides, LDO produced by calcination had large surface area and high metal dispersion. Based on this advantage, LDO is applicable to the removal of TPP due to the surface adsorption sites on LDO.

The objectives of this research were particularly to understand TPP removal behavior and the removal mechanism for Fe-LDO and Al-LDO through analyzing the structure of solid materials and composition of aqueous solution.

## 2. Materials and methods

### 2.1. Chemicals

Chemicals used in the experiment include sodium triphosphate (STPP,  $\text{Na}_3\text{P}_3\text{O}_{10}$ ), magnesium chloride · 6H<sub>2</sub>O ( $\text{MgCl}_2 \cdot 6\text{H}_2\text{O}$ ), calcium chloride ( $\text{CaCl}_2$ ), ferric chloride ( $\text{FeCl}_3$ ), aluminum chloride ( $\text{AlCl}_3$ ) and sodium hydroxide (NaOH). All reagents were purchased from Sigma-Aldrich Co., USA. Oxygen-free and decarbonated water was used for all synthesis and treatment processes under ambient conditions.

### 2.2. Preparation and characterization of Fe-LDO and Al-LDO

$\text{Mg}_{2-x}\text{Ca}_x\text{Fe}$  layered double hydroxide (Al-LDH,  $x=0.0\text{--}2.0$ ) was synthesized by co-precipitation method [14,15]. For example, the preparation of Ca-Fe-LDH is as follows. In brief, 50 mmol of  $\text{CaCl}_2$  and 20 mmol of  $\text{FeCl}_3$  were dissolved in 50 mL of water. This mixed salt solution was slowly added into 100 mL of an alkaline solution that contained 120 mmol of NaOH under vigorous magnetic stirring for 30 min. The suspension was aged at 25°C for 18 h under stirring. The precipitate was then separated by centrifugations and washed twice. The LDH was obtained after dried at 60°C.

The synthesis of  $\text{Mg}_{2-x}\text{Ca}_x\text{FeCl-LDH}$  ( $x = 0.5\text{--}1.5$ ) also adopted the same method except replacing  $\text{CaCl}_2$  by  $\text{MgCl}_2$ , and different Mg/Ca molar ratios (1:3, 1:1 and 3:1) were applied. The  $[\text{Ca} + \text{Mg}]/\text{Fe}$  molar ratio was controlled as 2:1 at the same time. Similarly, the preparation method of Al-LDH was similar to Fe-LDH except for the Me(III) was replaced by  $\text{AlCl}_3$ .

All the LDH samples were calcined at 450°C for 4 h in muffle furnace to obtain the LDO.

### 2.3. The removal of TPP on LDO

The TPP removal was carried out in  $\text{Na}_5\text{P}_3\text{O}_{10}$  solutions (pH = 8) in an incubator (25°C and 200 rpm shaking). The dose of LDO was 0.02 g per 100 mL of polyphosphate solution in thermodynamics experiment. TPP in the initial concentration ranged from 0 to 45 mg/L (total phosphorus, TP). Response time was 24 h. Particularly, when the initial (TP) was 0, the thermodynamics behavior of the LDO hydrolysis was recorded. The amount of TPP removal was calculated by using the following formula:

$$[\text{TPP}] \text{ (mg/g)} = ([\text{TP}]_0 - [\text{TP}]_e)/S \quad (1)$$

where [TPP] is the amount of TPP removal (mg/g);  $[\text{TP}]_0$  and  $[\text{TP}]_e$  are the initial and equilibrium concentrations of TPP (mg/L), respectively;  $S$  is the solid dosing (g/L; Table S1).

### 2.4. Analytical methods

The portable pH meter-installed glass electrode (Aqua Cond/pH, TPS) was used to measure pH. [TP] were determined using an ultraviolet–visible spectrophotometer (UV-2450, Shimadzu, Japan) measuring the absorbance at 700 nm [7]. Prior to the test, the sample was digested at 140°C (oil bath) in the presence of 5% (w/w)  $\text{K}_2\text{S}_2\text{O}_8$  solution, which promoted TPP converted into soluble  $\text{PO}_4^{3-}$  entirely [15]. Hence, [TP] could represent the actual TPP concentration.

The content of metal (Mg, Ca, Fe, Al) was determined with inductively coupled plasma atomic emission spectrometer (ICP-AES, Prodigy, Leeman Co., USA).

The X-ray diffraction analysis (XRD) for the solid sample was conducted on Miniflex (Rigaku), with Co  $K\alpha$  radiation ( $\lambda = 0.1789$  nm) at 40 kV, scanning speed controlled  $2^\circ \text{ min}^{-1}$  ( $2\theta$ ).

Thermal gravity (TG) profile of each sample with the corresponding mass spectroscopy (MS) profile of the evolved gaseous water ( $m/z = 18$ ) was collected on NETZSCH, Germany, Simultaneous TG-DTA-MS instrument (Apparatus STA 449C-Jupiter-QMS 403C Aeolos) in air atmosphere at a ramping rate of 5°C/min from 35°C to 500°C.

## 3. Results and discussion

### 3.1. LDO formation in thermal treatment

As the LDO is prepared from LDH, suggested that the structure of LDO is relative to its precursor LDH during calcination. Fig. 1 illustrates the weight loss of LDH during the heating. In TG profiles of Fe-LDH, there were two mass loss steps during temperature increasing to 500°C. The first mass

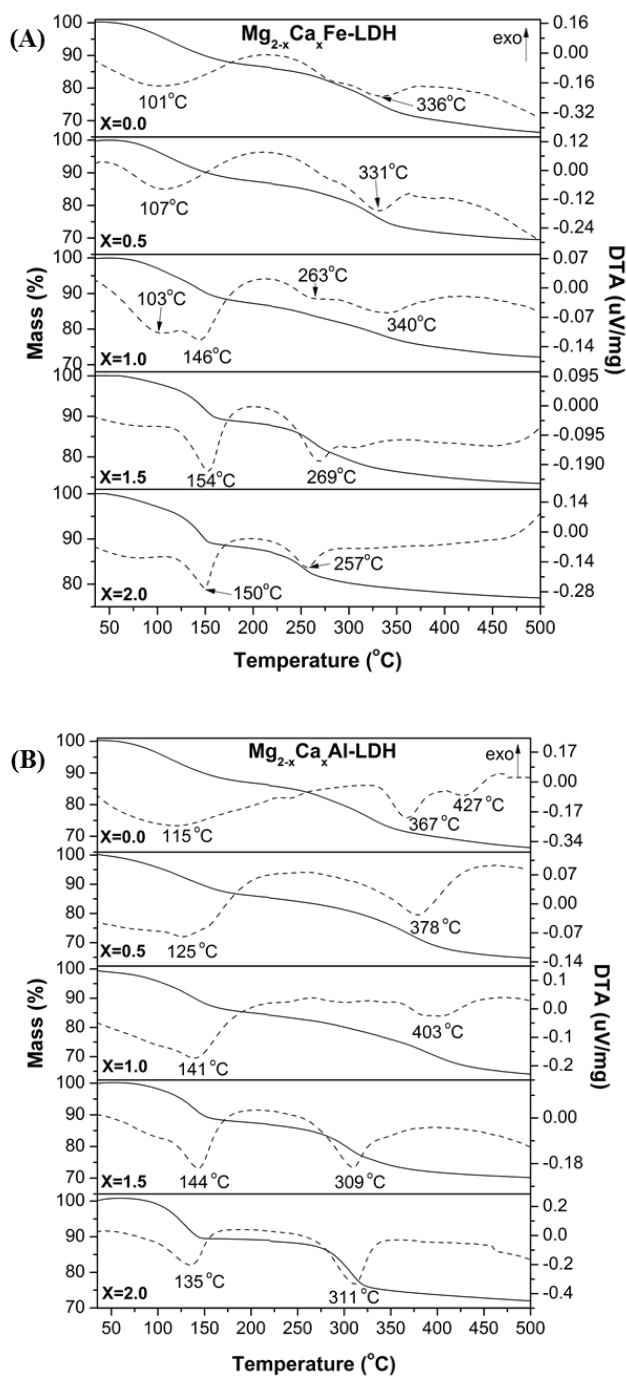


Fig. 1. TGA curves of Mg<sub>2-x</sub>Ca<sub>x</sub>Fe-LDH (A) and Mg<sub>2-x</sub>Ca<sub>x</sub>Al-LDH (B) ( $x = 0.0$ – $2.0$ ).

loss of 12%–15% happened before 200°C–250°C due to the loss of the water in the LDH interlayer. The second mass loss of 10%–18% was observed after 250°C, which can be assigned to the OH loss in the brucite-like layer of LDH [25]. Both steps were endothermic and were recorded in DTA curves. The DTA curve of Mg<sub>2</sub>FeCl-LDH shows two endothermic peaks at 101°C for dehydration and 336°C for dehydroxylation. It is noted that the corresponding endothermic peak in the DTA curve of Ca<sub>2</sub>FeCl-LDH was recorded at 150°C and 257°C,

respectively. Ca in LDH layers can increase the affinity of H<sub>2</sub>O to the LDH interlayer and therefore weakened the binding of OH-(M(II)Fe) [26]. Accordingly, Ca in LDH was responsible for the higher dehydration temperature and the lower dehydroxylation temperature than Mg<sub>2</sub>FeCl-LDH. Therefore, different temperature of water loss in thermal gravity analysis (TGA) curves of Ca<sub>2</sub>FeCl-LDH and Mg<sub>2</sub>FeCl-LDH reflects the difference in the feature structure of the LDHs.

When a portion of Mg was replaced by Ca in Fe-LDH, the structure of LDH was changed. In Fig. 1(A), the DTA curve of LDH (Mg<sub>2-x</sub>Ca<sub>x</sub>Fe-LDH) at  $x = 0.5$  and  $x = 1.5$  is similar to that of Mg<sub>2</sub>FeCl-LDH and Ca<sub>2</sub>FeCl-LDH, respectively. This reflected that the Mg-Fe-LDH structure was predominant in Mg<sub>1.5</sub>Ca<sub>0.5</sub>Fe-LDH while Ca-Fe-LDH structure in Mg<sub>0.5</sub>Ca<sub>1.5</sub>Fe-LDH. It is noted that there were four endothermic peaks in the DTA curve of LDH at  $x = 1.0$ . Apparently, the endothermic peaks at 103°C and 340°C indicated the Mg-Fe-LDH structure while those at 146°C and 263°C reflected the Ca-Fe-LDH. This suggested that both Mg<sub>2</sub>FeCl-LDH and Ca<sub>2</sub>FeCl-LDH were coexisted at  $x = 1.0$ , but not a uniformed Mg-Ca-Fe-LDH structure.

In comparison, the similar thermal analysis profiles were observed in most Mg<sub>2-x</sub>Ca<sub>x</sub>Al-LDH samples. In Fig. 1(B), TG curves of all Al-LDHs illustrate the two main mass loss processes, which can be assigned to dehydration step at low temperature and dehydroxylation step at high temperature. Moreover, DTA curves of Mg<sub>2-x</sub>Ca<sub>x</sub>Al-LDH samples at  $x = 0.0$ – $1.0$  show the endothermic peak of H<sub>2</sub>O evaporation at 115°C–141°C and the other one of OH evaporation at 367°C–403°C. In the samples at  $x > 1.0$ , the dehydration peak in DTA curve was around 135°C–144°C, whereas the dehydroxylation peak was at 309°C–311°C. This observation revealed that Mg-Al-LDH structure was predominant at  $x < 1.0$  and Ca-Al-LDH structure was the main composition at  $x > 1.0$ . Interestingly, at  $x = 1.0$ , the structure of Mg<sub>1.0</sub>Ca<sub>1.0</sub>Al-LDH was close to that samples at  $x < 1.0$ , which showed that a uniformed Mg-Ca-Al-LDH structure was formed when Ca was doped into the framework.

Accordingly, it is supposed that after calcination, the separated Ca-Fe-LDH and Mg-Fe-LDH structure in ternary Fe-LDH resulted in the mixture of Ca-Fe and Mg-Fe oxides formation. In contrast, Mg-Ca-Fe oxide would be formed after the calcination of ternary Al-LDH.

Table 1 lists the mass loss after calcination at 450°C in a batch test. Compared with that in TGA characterization, the weight loss of all LDHs was consistent with the thermal analysis result. Accordingly, the calcination temperature was set at 450°C for the LDO sample preparation as a complete water loss can be achieved.

### 3.2. Removal of TPP by LDO

Fig. 2 shows the removal profiles of TPP on Fe-LDO and Al-LDO (calcined at 450°C). Among all samples of Fe-LDO (Fig. 2(A)), the TPP removal amount increased sharply when the equilibrium concentration of TPP was less than 3 mg/L. The TPP removal amount reached constant with the equilibrium concentration of TPP increasing. It is observed that the final TPP removal amount was relative to the value of  $x$  in Mg<sub>2-x</sub>Ca<sub>x</sub>Fe-LDO. At  $x = 0.0$ , the TPP removal amount was 11.8 mg/g (as total P). The increase in the value of  $x$  to 1.5

Table 1  
The comparison between the mass loss and data of thermal analysis after calcination

Samples	Mass loss (%)	
	Calcination	Thermal analysis
Mg <sub>2</sub> Al-LDO	32	32
Mg <sub>1.5</sub> Ca <sub>0.5</sub> Al-LDO	34	34
Mg <sub>1.0</sub> Ca <sub>1.0</sub> Al-LDO	33	34
Mg <sub>0.5</sub> Ca <sub>1.5</sub> Al-LDO	29	29
Ca <sub>2</sub> Al-LDO	26	27
Mg <sub>2</sub> Fe-LDO	36	33
Mg <sub>1.5</sub> Ca <sub>0.5</sub> Fe-LDO	31	30
Mg <sub>1.0</sub> Ca <sub>1.0</sub> Fe-LDO	30	27
Mg <sub>0.5</sub> Ca <sub>1.5</sub> Fe-LDO	27	26
Ca <sub>2</sub> Fe-LDO	24	23

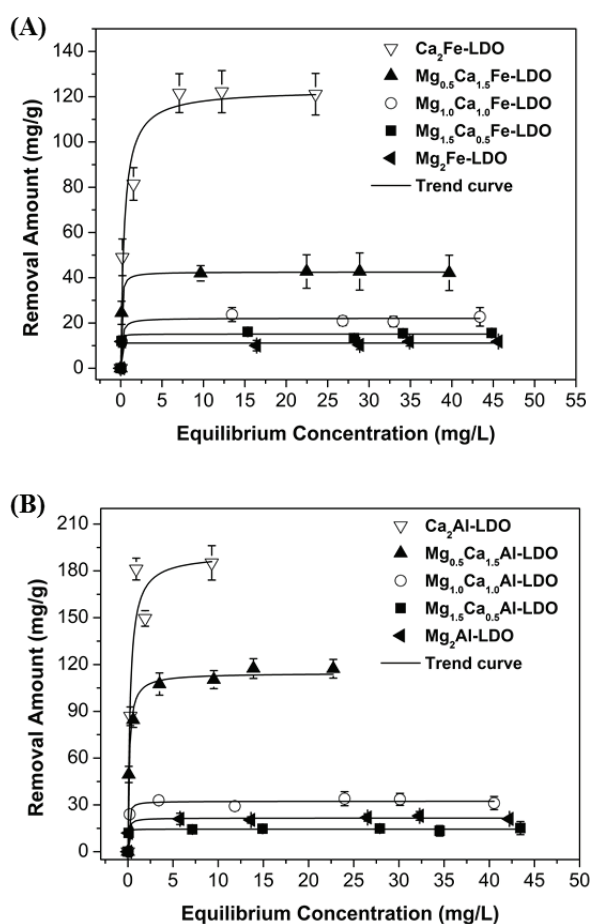


Fig. 2. TPP thermodynamic behavior on Mg<sub>2-x</sub>Ca<sub>x</sub>Fe-LDO (A) and Mg<sub>2-x</sub>Ca<sub>x</sub>Al-LDO (B) ( $x = 0.0-2.0$ ).

slightly improved the TPP removal amount as it ranged from 15.6 to 42.2 mg/g. At  $x = 2.0$ , the TPP removal amount was 121 mg/g, three times higher than that at  $x = 1.5$ . It implied that Ca in the Fe-LDO was predominantly responsible for the TPP removal. Moreover, Fig. 2(B) illustrates the similar TPP removal on Al-LDO. The TPP removal isotherm showed a

low TPP removal amount at 15.1–31.2 mg/g with the increasing of  $x$  from 0.0 to 1.0 while that at  $x = 2.0$  were 185 mg/g. It is interesting that the TPP amount of Mg<sub>0.5</sub>Ca<sub>1.5</sub>Al-LDO ( $x = 1.5$ ) was 117 mg/g, over three times higher than that on Al-LDO at a relatively low  $x$  value. This indicated that the TPP removal was contributed to the TPP adsorption induced by the LDH structure rather than Ca content.

Tables 2 and 3 list the concentration of metal ions in the solution after the TPP removal by Mg<sub>2-x</sub>Ca<sub>x</sub>Fe-LDO and Mg<sub>2-x</sub>Ca<sub>x</sub>Al-LDO, respectively. In both cases of Fe-LDO and Al-LDO, Mg concentration in the residual solution decreased from 0.6 to 0 mmol/L with the decreasing in the value of  $x$ , while that of Ca increased to 0.47 mmol/L correspondingly. It is interesting that no Fe was detected in the solution after the TPP removal on Mg<sub>2-x</sub>Ca<sub>x</sub>Fe-LDO, while Al was released after the TPP removal on Mg<sub>2-x</sub>Ca<sub>x</sub>Al-LDO. With the value of  $x$  increased, the Al concentration was ranged from 0.1 to 0.7 mmol/L. The leached Al indicated that a portion of Al-LDO was dissolved, which was contributed to the Al(OH)<sub>4</sub><sup>-</sup> derived from LDO at the final pH over 10.0 (Table S2). Table 3 lists the molar ratio of metals in Al-LDO. The Ca/Mg ratio was ranged from 0.12 to 1.57, lower than the designed ratio (Table 3). The similar proportion was also observed in Fe-LDO (Table 2). The low Ca content in LDO was relative to the corresponding LDH precursor. Moreover, the Me(II)/Me(III) in both LDOs was close to 2.0, which was also observed in pure LDH. It seemed that LDH recovery would be achieved when LDO was in TPP solution. In the case of Fe-LDO, the Fe content in residue increased, which resulted in a low molar ratio of bivalent metal to total metal ( $R$ ). The similar situation was observed in the case of Al-LDO. However,  $R$  in Al-LDO residue was close to the range of that in LDH (0.25–0.4) while was lower in Fe-LDO residue. Due to the reformation effect of LDH, it is proposed that Al-LDH was reconstructed in the case of Al-LDO after TPP removal. This is probably responsible for the high TPP removal in Mg<sub>0.5</sub>Ca<sub>1.5</sub>Al-LDO.

### 3.3. Physicochemical features of LDO samples before and after TPP removal

Fig. 3 shows the XRD pattern of the product of Mg<sub>2-x</sub>Ca<sub>x</sub>Fe-LDH after calcination ( $x = 0.0-2.0$ , at 450°C), the diffraction peak of sharp spinel phase MgO and MgFe<sub>2</sub>O<sub>4</sub> ( $2\theta = 35.1^\circ, 41.4^\circ, 50.4^\circ, 63.0^\circ, 67.3^\circ$  and  $74.1^\circ$ ) mainly existed in C-Mg<sub>2</sub>Fe-LDH. No spinel structure-like product was observed in C-Ca<sub>2</sub>Fe-LDO. This seems that the dehydration of LDH did not lead to the formation of the complex oxides of CaFe(O) (Ca<sub>x</sub>Fe<sub>y</sub>O<sub>(2x+3y)/2</sub>), which was a possible product from high-temperature calcination of CaAlCl-LDH [27]. In addition, CaCO<sub>3</sub> was indexed in products as a small diffraction peak at  $34.5^\circ(2\theta)$  was recorded. In C-MgCaFe-LDH, the XRD diffraction patterns of MgO and MgFe<sub>2</sub>O<sub>4</sub> gradually decreased with the increase of Ca content. Meanwhile, the emerge of the diffraction peak of Ca<sub>x</sub>Fe<sub>y</sub>O<sub>(2x+3y)/2</sub> further proved the formation complex oxides of Ca with Fe.

Fig. 4 shows that the main product of Mg<sub>2</sub>Al-LDO after calcination was MgAl(O) complex oxides [28]. In Ca<sub>2</sub>Al-LDO, it showed that there was poor crystallinity of CaAlO complex oxides (Ca<sub>12</sub>Al<sub>14</sub>O<sub>33</sub>) and a certain amount of CaO due to the existence of broad peak on ( $2\theta = 30^\circ-50^\circ$ ) [27, 29]. Due to the lower heating temperature, it was more difficult to form

a high degree of crystallization of CaAlO composite oxides [29]. For the calcination product of MgCaAl-LDO, with the increase of Ca content in MgCaAl-LDH, MgAl(O) complex oxides gradually transformed to CaAl(O) composite oxides.

Fig. 5 shows that the XRD of Fe-LDO products after TPP removal. In most cases, there were the diffraction peaks of spinel phase MgO and MgFe<sub>2</sub>O<sub>4</sub>. This indicated that the recovery of LDH did not happen in the structure of Mg-Fe-O system as the spinel structure of Mg-Fe-O was more stable than the composite oxides of Mg-Al-O [30]. Meanwhile, the diffraction peak of spinel phase was weak with the decreasing of the Ca content. When Ca was predominant in the LDO ( $x = 1.5$  and  $2.0$ ), CaCO<sub>3</sub> ( $2\theta = 34.4^\circ$ ) was observed. This is probably contributed to Fe-O amorphous structure that was left by the dissolution of Ca from the CaFe(O) structure during TPP removal [15]. As the high content of Ca in the original LDH mixture, the dissolution of Ca led to low amount of bivalent metal in LDO, which resulted in the failure of LDH reformation. This was probably the reason why the TPP removal amount on Mg<sub>0.5</sub>Ca<sub>1.5</sub>Fe-LDO (40 mg P/g) was lower than that on Mg<sub>0.5</sub>Ca<sub>1.5</sub>Fe-LDH (84.2 mg P/g) [15]. On the other hand, the Ca releasing was responsible for the TPP removal, which was similar to the situation in the phosphate removal on Ca-LDH [31]. Accordingly, it is proposed that the TPP removal on Fe-LDO was mainly attributed to the surface adsorption of the MgFe-LDH and precipitation of Ca.

In comparison, the high TPP removal is probably relative to the reformation effect in Al-LDO product. In Fig. 6, the XRD pattern of P-Mg<sub>x</sub>Al-LDO samples shows that the diffraction peaks at  $13.3^\circ$ ,  $27.1^\circ$ ,  $40.7^\circ$ ,  $46.1^\circ$ ,  $54.8^\circ$ ,  $72.3^\circ$  and  $73.5^\circ$  ( $2\theta$ ), indexed as the typical reflection planes of hydroxalite-like structure. The LDH structure in the solid samples after TPP removal indicates the reformation effect occurred in MgAl(O) system. However, the basal space (0.77 nm) observed in the resultant was in accordance with Cl<sup>-</sup> intercalated LDH [16]. As the removal capacity (28 mg P/g) was

lower than that of Mg<sub>2</sub>Al-LDH (40 mg P/g), it is suggested that TPP was adsorbed onto the surface (or edges) instead of intercalated into the hydroxide layers [14]. In addition, the broad peak revealed the formation of amorphous Ca-TPP precipitate, which indicated that removal of TPP by Ca<sub>2</sub>Al-LDO mainly relied on precipitation of Ca with TPP.

Due to the reformation effect, the XRD pattern of P-Mg<sub>1.5</sub>Ca<sub>0.5</sub>Al-LDO and P-Mg<sub>1.0</sub>Ca<sub>1.0</sub>Al-LDO also showed the hydroxalite-like structure. It is noted that the LDH structure of P-Mg<sub>0.5</sub>Ca<sub>1.5</sub>Al-LDO was weaker than that of the other two LDOs after TPP removal, which indicated that amorphous structure was dominated in the product. Besides, the TPP removal amount on Mg<sub>0.5</sub>Ca<sub>1.5</sub>Al-LDO (120 mg P/g) was higher than that on other ternary Al-LDOs, even higher than

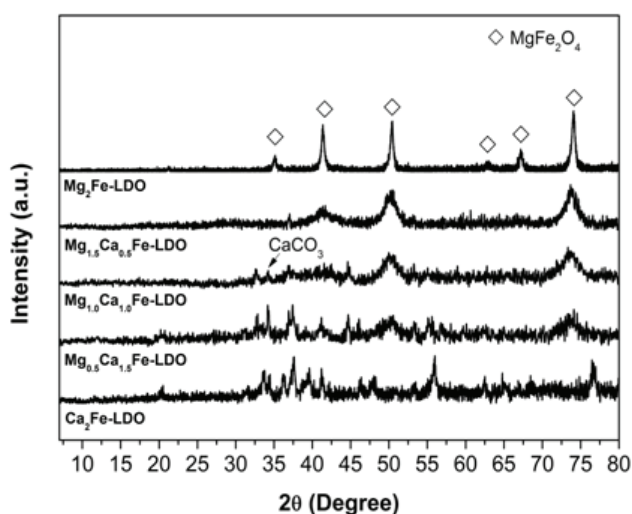


Fig. 3. XRD patterns for the synthesized Mg<sub>2-x</sub>Ca<sub>x</sub>Fe-LDO ( $x = 0.0-2.0$ ).

Table 2

Practical molar ratio of Mg/Ca/Fe in Fe-LDO, and metal ion concentration in solution after TPP removal

Sample	Practical molar ratio of Mg/Ca/Fe in Fe-LDO		Cations in solution after TPP removal (mmol/L)		
	Ca/Mg	M(II)/Fe	Mg	Ca	Fe
Mg <sub>2</sub> Fe-LDO	/	1.92	0.60	0.00	0.01
Mg <sub>1.5</sub> Ca <sub>0.5</sub> Fe-LDO	0.12	1.73	0.45	0.11	0.00
Mg <sub>1.0</sub> Ca <sub>1.0</sub> Fe-LDO	0.65	1.81	0.14	0.39	0.00
Mg <sub>0.5</sub> Ca <sub>1.5</sub> Fe-LDO	1.54	1.86	0.07	0.47	0.00
Ca <sub>2</sub> Fe-LDO	/	1.91	0.00	0.47	0.00

Table 3

Practical molar ratio of Mg/Ca/Al in Al-LDO, and metal ion concentration in solution after TPP removal

Sample	Practical molar ratio of Mg/Ca/Al in Al-LDO		Cations in solution after TPP removal (mmol/L)		
	Ca/Mg	M(II)/Al	Mg	Ca	Al
Mg <sub>2</sub> Al-LDO	/	1.81	0.47	0.00	0.10
Mg <sub>1.5</sub> Ca <sub>0.5</sub> Al-LDO	0.12	1.69	0.42	0.12	0.12
Mg <sub>1.0</sub> Ca <sub>1.0</sub> Al-LDO	0.66	1.82	0.18	0.47	0.22
Mg <sub>0.5</sub> Ca <sub>1.5</sub> Al-LDO	1.57	1.87	0.05	0.47	0.56
Ca <sub>2</sub> Al-LDO	/	2.01	0.00	0.37	0.71

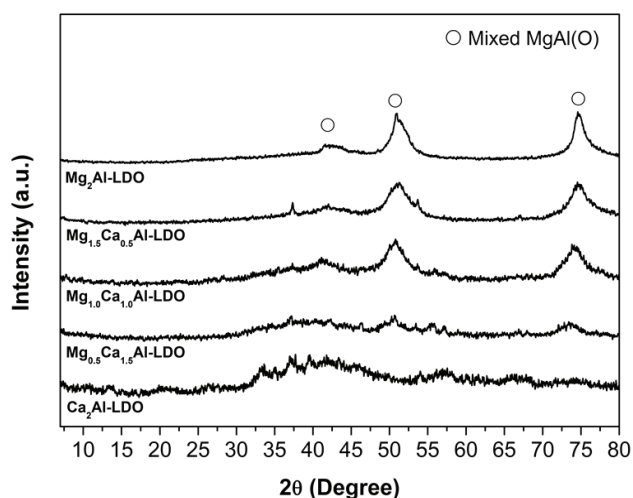


Fig. 4. XRD patterns for the synthesized  $Mg_{2-x}Ca_xAl-LDO$  ( $x = 0.0-2.0$ ).

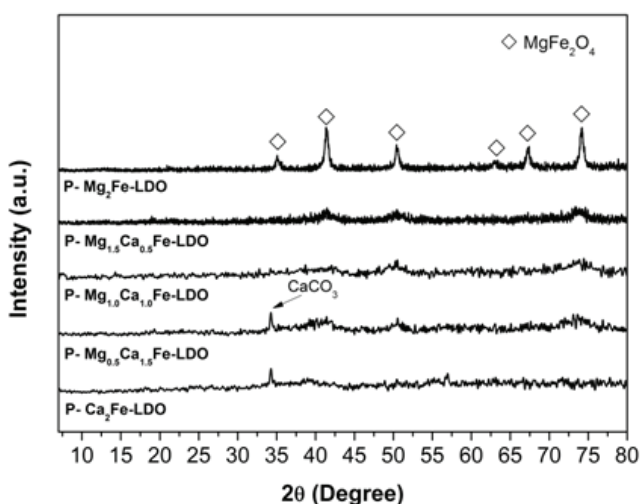


Fig. 5. The XRD of  $Mg_{2-x}Ca_xFe-LDO$  ( $x = 0.0-2.0$ ) product after removing TPP.

that on  $Mg_{0.5}Ca_{1.5}Al-LDH$  (80 mg P/g) [14]. Considering the well-dispersion of Ca in the original Mg-Al-LDH structure, the high TPP removal amount is probably relative to the amorphous Mg-Al-LDH framework after Ca release. In addition, the formation of  $CaCO_3$  ( $2\theta = 34.2^\circ$ ) in the products was recorded. This was attributed to the combination of dissociative  $Ca^{2+}$  and dissociative  $CO_3^{2-}$  in solution.

### 3.4. Removal mechanism

For Fe-LDO and Al-LDO, the TPP removal mechanism is the synergistic effect of structural adsorption and Ca-induced precipitation. In Fe-LDO, the final solution pH is between 9.9 and 10.8 (Table S2) due to the partial dissolution of metal oxides (Table 2). For instance, in  $Mg_2Fe-LDO$ , 0.60 mmol/L Mg revealed the dissolution of 26% Mg in solution (Table 2). Nevertheless, no Fe was detected in solution, in accordance with the higher stability  $K_{sp}$  of iron(III) oxide. Only 11.8 mg/g

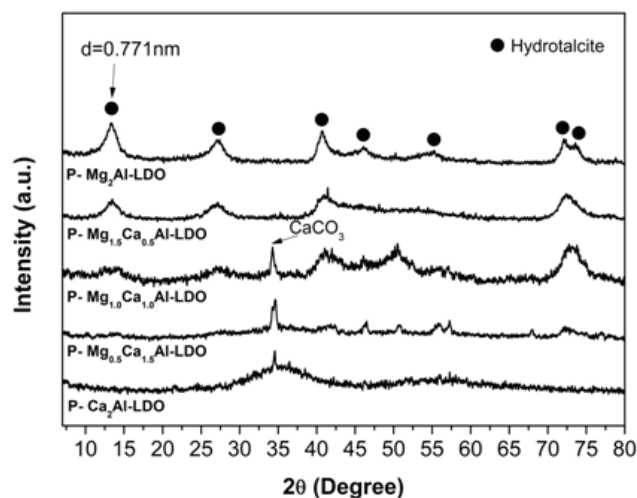


Fig. 6. The XRD of  $Mg_{2-x}Ca_xAl-LDO$  ( $x = 0.0-2.0$ ) product after removing TPP.

LDO TPP has been removed, and Mg and Fe still existed in the form of oxides in  $Mg_2Fe-LDO$ . It could be inferred that the  $Mg_2Fe-LDO$  removal of TPP rely on the surface adsorption. On the contrary, in Ca case, as the difference in the XRD pattern of solid samples before and after the TPP removal (Figs. 3 and 5), the dissolution of Ca from  $Ca_2Fe-LDO$  led to TPP removal in the form of Ca-TPP ( $Ca_5(P_3O_{10})_2 \cdot nH_2O$ ). The Ca concentration was 0.47 mmol/L in the solution after TPP removal (Table 2), suggesting that there was 29% of Ca leaching out from the original  $Ca_2Fe-LDO$ . As TPP removal amount was 121 mg/g LDO, the consumption of Ca is 40% of total Ca. This indicates that 44% of residual Ca in P- $Ca_2Fe-LDO$  was not used for removing the TPP. Comparing with that in P- $Ca_2Fe-LDH$  [15], Ca in P- $Ca_2Fe-LDO$  may be retained within the framework of Fe-O.

In the system of  $Mg_{2-x}Ca_xFe-LDO$ , with the increasing of  $x$  value, TPP removal amount increased and the Mg dissolved amount decreased. As shown in Table 2, with the  $x$  value from 0.5 to 1.5, the proportion of dissolved Mg in total Mg decreased from 26% to 10%. This indicates that MgO gradually decreased in Mg-Fe-O mixed oxides, which led to the decreasing in the dissolved Mg. The residual Mg was probably in the structure of  $MgFe_2O_4$ . As Mg content was higher than Ca content in both  $Mg_{1.5}Ca_{0.5}Fe-LDO$  and  $Mg_{1.0}Ca_{1.0}Fe-LDO$ , the main phase was existed as Mg-Fe-O. Similar to that in  $Mg_2Fe-LDO$ , TPP removal was mainly responsible for the surface adsorption both in  $Mg_{1.5}Ca_{0.5}Fe-LDO$  and  $Mg_{1.0}Ca_{1.0}Fe-LDO$ . Different from the dissolution of Mg, the proportion of dissolved Ca drawn near 50% both in  $Mg_{1.5}Ca_{0.5}Fe-LDO$  and  $Mg_{1.0}Ca_{1.0}Fe-LDO$ , 30% in  $Mg_{0.5}Ca_{1.5}Fe-LDO$ , respectively. With the increasing of  $x$  value, Ca concentration in the solution decreased. It was reported that the bond strength of OH to metal oxide increased with increasing  $x$  in  $Mg_{3-x}Ca_xFe-LDH$  [32]. As the surface adsorption on LDH involved the exchange with OH groups, the weaker affinity of OH bond in MgCaFe-LDH after Ca dissolution at  $x > 1$  was responsible for the bigger adsorption capacities on MgCaFe-O structure, compared with the case at  $x < 1$ . Accordingly, this indicates that the removal of TPP on  $Mg_{0.5}Ca_{1.5}Fe-LDO$  was contributed to the precipitation of  $Ca_5(P_3O_{10})_2 \cdot nH_2O$  apart from the

surface adsorption of Mg-Fe-O. Moreover, it revealed that there were 15% Ca transferred into the residue during the removal, which demonstrated that the TPP removal amount was approximately 30 mg/g LDO. Considering the structure of Mg-Fe-O adsorbing capacity of TPP (10–20 mg/g LDO), the total removal amount could reach 40–50 mg/g LDO, which was closer to the actual value. Therefore, a moderate amount of dissolved Ca could induce a synergistic effect for the removal of TPP using  $Mg_{0.5}Ca_{1.5}Fe-LDO$ .

Besides, Al-LDO product has a reformation effect during the removal. It was suggested that the Al-rich ternary LDHs could be used as absorbents to remove TPP. As shown in Table S2, the final pH was 10.1 after TPP removal on  $Mg_2Al-LDO$ , close to that in the case of  $Ca_2Al-LDO$  (10.8). Mg and Ca concentration after TPP removal was closer to that in Fe-LDO. Based on the TPP removing under similar conditions to that in Fe-LDH, it was proposed that TPP removal mainly relied on the surface adsorption and edge intercalation effect of the recovery LDH structure in  $Mg_2Al-LDO$ , while the Ca precipitation in  $Ca_2Al-LDO$ . In addition, based on the high TPP removal amount, the residual rate of Ca is 71% and 81% both in  $Ca_2Fe-LDO$  and  $Ca_2Al-LDO$ , respectively. The similar result was also found in the removal of phosphate on Ca-Al-LDH [33]. It could be inferred that there was more the dissolution of Ca in  $Ca_2Al-LDO$  and formed the precipitation of  $Ca_5(P_3O_{10})_2 \cdot nH_2O$ .

Similar to the situation in the case of  $Mg_{2-x}Ca_xFe-LDO$ , the final pH value increased to about 9.9 to 10.7 (Table S2) with the metal dissolved in Al-LDO. Meanwhile, with the increasing of  $x$  value, the proportion of dissolved Mg gradually decreased. It means that the percentage of Mg increased from 79% to 94% in  $Mg_{1.5}Ca_{0.5}Al-LDO$  and  $Mg_{0.5}Ca_{1.5}Al-LDO$  (Table 3), which was higher than in  $Mg_{2-x}Ca_xFe-LDO$ . As the results of XRD (Fig. 6), the dissolution of Mg decreased due to the formation of Mg-Al-LDH. Correspondingly, the dissolution of Ca gradually increased with the  $x$  value increased. According to the concentration of Ca in the solution (Table 3), the retention rate of Ca was about 50% in both P- $Mg_{1.5}Ca_{0.5}Al-LDO$  and P- $Mg_{1.0}Ca_{1.0}Al-LDO$ , similar to that in P- $Mg_{1.5}Ca_{0.5}Fe-LDO$  and P- $Mg_{1.0}Ca_{1.0}Fe-LDO$ . Accordingly, the low Ca content in LDO indicated that the TPP removal was mainly contributed to the adsorption of Mg-Al-LDH, which was the main phase after the reformation of LDH from LDO. In comparison, the retention rate of Ca is 63% in P- $Mg_{0.5}Ca_{1.5}Al-LDO$ . As 117 mg/g LDO of TPP removal, the high retention rate of Ca indicated that the TPP removal was probably attributed to Ca in the Mg-Al-LDH framework, which resulted in the formation of  $Ca_5(P_3O_{10})_2 \cdot nH_2O$  precipitation. Therefore, the reformation effect of Al-LDO product significantly increased the adsorption quantity of TPP.

#### 4. Conclusion

In this research, we investigated the removal of TPP using LDO ( $Mg_{2-x}Ca_xFe-LDO$  and  $Mg_{2-x}Ca_xAl-LDO$ ,  $x = 0.0-2.0$ ) derived from LDH by calcination. The TPP removal behavior in Al-LDO was similar to that in Fe-LDO. It was revealed that TPP was removed predominantly either via the surface adsorption or Ca-TPP precipitation. Nevertheless, the sorption amount in Al-LDO of TPP was higher compared with Fe-LDO. This was mainly because Al-LDO could

be reverted to LDH structure and adsorbed TPP. Specially, the elemental analysis (ICP-AES) of the aqueous solution and the solid materials suggested that the synergy of the sorption and precipitation occurred on  $Mg_{0.5}Ca_{1.5}Fe-LDO$ , but not on  $Mg_{0.5}Ca_{1.5}Al-LDO$ . Therefore, our results provide a feasible approach for the anionic contaminants removal by LDO.

#### Acknowledgments

This project is supported by National Nature Science Foundation of China (no. 20877053, no. 51174132 and no. 21207086), and Shanghai Municipal Education Commission Innovation project (2015). We also appreciate the technical support from Instrumental Analysis & Research Center of Shanghai University.

#### References

- [1] Z. Zhang, H. Li, J. Zhu, L. Weiping, X. Xin, Improvement strategy on enhanced biological phosphorus removal for municipal wastewater treatment plants: full-scale operating parameters, sludge activities, and microbial features, *Bioresource Technol.*, 102 (2011) 4646–4653.
- [2] M.W. Lai, A.N. Kulakova, J.P. Quinn, J.W. McGrath, Stimulation of phosphate uptake and polyphosphate accumulation by activated sludge microorganisms in response to sulfite addition, *Water Sci. Technol.*, 63 (2011) 649–653.
- [3] D.J. Halliwell, I.D. McKelvie, B.T. Hart, R.H. Dunhill, Hydrolysis of triphosphate from detergents in a rural waste water system, *Water Res.*, 35 (2001) 448–454.
- [4] F. Rashchi, J.A. Finch, Polyphosphates: a review their chemistry and application with particular reference to mineral processing, *Miner. Eng.*, 13 (2000) 1019–1035.
- [5] J.R. Van Wazer, E.J. Griffith, J.F. McCullough, Hydrolysis of condensed phosphates, *J. Am. Chem. Soc.*, 74 (1952) 4977–4978.
- [6] L.O. Torres-Dorante, N. Claassen, B. Steingrobe, H.W. Olf, Fertilizer-use efficiency of different inorganic polyphosphate sources: effects on soil P availability and plant P acquisition during early growth of corn, *J. Plant Nutr. Soil Sci.*, 169 (2006) 509–515.
- [7] APHA, Standard methods for the examination of water and wastewater, 18th Ed., American Public Health Association, Washington, D.C., 1992.
- [8] L.E. de-Bashan, Y. Bashan, Recent advances in removing phosphorus from wastewater and its future use as fertilizer (1997–2003), *Water Res.*, 38 (2004) 4222–4246.
- [9] R. Chitrakar, A. Sonoda, Y. Makita, T. Hirotsu, Selective Uptake of Phosphate Ions from Sea Water on Inorganic Ion-Exchange Materials, J.A. Daniels, Ed., *Advances in Environmental Research*, Nova Science Publishers Inc., New York, 2011, pp. 119–152.
- [10] X.H. Guan, G.H. Chen, C. Shang, Adsorption behavior of condensed phosphate on aluminum hydroxide, *J. Environ. Sci.*, 19 (2007) 312–318.
- [11] J. Zhou, S. Yang, J. Yu, Facile fabrication of mesoporous MgO microspheres and their enhanced adsorption performance for phosphate from aqueous solutions, *Colloids Surf. A*, 379 (2011) 102–108.
- [12] Y.Y. Wu, Y. Yu, J.Z. Zhou, J.Y. Liu, Y. Chi, Z.P. Xu, G.R. Qian, Effective removal of pyrophosphate by Ca-Fe-LDH and its mechanism, *Chem. Eng. J.*, 179 (2012) 72–79.
- [13] D.J. Jeon, S.H. Yeom, Recycling wasted biomaterial, crab shells, as an adsorbent for the removal of high concentration of phosphate, *Bioresource Technol.*, 100 (2009) 2646–2649.
- [14] J.Z. Zhou, Z.P. Xu, S.Z. Qiao, J.Y. Liu, Q. Liu, Y.F. Xu, J. Zhang, G.R. Qian, Triphosphate removal processes over ternary CaMgAl-layered double hydroxides, *Appl. Clay Sci.*, 54 (2011) 196–201.

- [15] J.Z. Zhou, Z.P. Xu, S.Z. Qiao, Q. Liu, Y.F. Xu, G.R. Qian, Enhanced removal of triphosphate by MgCaFe-Cl-LDH: synergism of precipitation with intercalation and surface uptake, *J. Hazard. Mater.*, 189 (2011) 586–594.
- [16] J.Z. Zhou, L.L. Feng, J. Zhao, J.Y. Liu, Q. Liu, J. Zhang, G.R. Qian, Efficient and controllable phosphate removal on hydrocalumite by multi-step treatment based on pH-dependent precipitation, *Chem. Eng. J.*, 185–186 (2012) 219–225.
- [17] G.R. Qian, L.L. Feng, J.Z. Zhou, Y.F. Xu, J.Y. Liu, J. Zhang, Z.P. Xu, Solubility product ( $K_{sp}$ )-controlled removal of chromate and phosphate by hydrocalumite, *Chem. Eng. J.*, 181–182 (2012) 251–258.
- [18] M.K. Ram Reddy, Z.P. Xu, G.Q. (Max) Lu, and J.C. Diniz da Costa, Effect of  $SO_x$  adsorption on layered double hydroxides for  $CO_2$  capture, *Ind. Eng. Chem. Res.*, 47 (2008) 7357–7360.
- [19] V.R.L. Constantino, T.J. Pinnavaia, Basic properties of  $Mg^{2+}$ - $Al^{3+}$  layered double hydroxides intercalated by carbonate, hydroxide, chloride, and sulfate anions, *Inorg. Chem.*, 34 (1995) 883–892.
- [20] M. Tsuji, M. Mao, T.Y.Y. Tamaura, Hydrotalcites with an extended  $Al^{3+}$ -substitution: synthesis, simultaneous TGA-DTA-MS study, and their  $CO_2$  adsorption behaviors, *J. Mater. Res.*, 8 (1993) 1137–1142.
- [21] Y. Kim, W. Yang, P.K.T. Liu, M. Shahimi, T.T. Tsotsis, Thermal evolution of the structure of a Mg-Al- $CO_3$  layered double hydroxide: sorption reversibility aspects, *Ind. Eng. Chem. Res.*, 43 (2004) 4559–4570.
- [22] S. Miyata, T. Hirose, Adsorption of  $N_2$ ,  $O_2$ ,  $CO_2$ , and  $H_2$  on hydrotalcite-like system:  $Mg^{2+}$ - $Al^{3+}$ -( $Fe(CN)_6$ ) $^{4-}$ , *Clays Clay Miner.*, 26 (1978) 441–447.
- [23] H. Pfeiffer, E. Lima, V. Lara, J.S. Valente, Thermokinetic study of the rehydration process of a calcined MgAl-layered double hydroxide, *Langmuir*, 26 (2010) 4074–4079.
- [24] P.S. Braterman, Z.P. Xu, F. Yarberry, Layered Double Hydroxides (LDHs), S.M. Auerback, K.A. Carrado, P.K. Dutta, Eds., *Handbook of Layered Materials*, Marcell Dekker, New York, 2004, pp. 373–474.
- [25] M.A. Aramendia, Y. Aviles, V. Borau, J.M. Luque, J.M. Marinas, J.R. Ruiz, F.J. Urbano, Thermal decomposition of Mg Al and Mg Ga layered-double hydroxides: a spectroscopic study, *J. Mater. Chem.*, 9 (1999) 1603–1607.
- [26] J. Zhang, Y.F. Xu, G.G. Qian, Z.P. Xu, C. Chen, Q. Liu, Reinvestigation of dehydration and dehydroxylation of hydrotalcite-like compounds through combined TG-DTA-MS analyses, *J. Phys. Chem. C*, 114 (2010) 10768–10774.
- [27] L. Vieille, I. Rousselot, F. Leroux, J.P. Besse, C. Taviot-Gueho, Hydrotalcite and its polymer derivatives. 1. Reversible thermal behavior of Friedel's salt: a direct observation by means of high-temperature in situ powder X-ray diffraction, *Chem. Mater.*, 15 (2003) 4361–4368.
- [28] R. Liu, R.L. Frost, W.N. Martens, Absorption of the selenite anion from aqueous solutions by thermally activated layered double hydroxide, *Water Res.*, 43 (2009) 1323–1329.
- [29] M.J. Campos-Molina, J. Santamaria-Gonzalez, J. Merida-Robles, R. Moreno-Tost, M.C.G. Albuquerque, S. Bruque-Gamez, E. Rodriguez-Castellon, A. Jimenez-Lopez, P. Maireles-Torres, Base catalysts derived from hydrocalumite for the transesterification of sunflower oil, *Energy Fuels*, 24 (2010) 979–984.
- [30] M. del Arco, P. Malet, R. Trujillano, V. Rives, Synthesis and characterization of hydrotalcites containing Ni(II) and Fe(III) and their calcination products, *Chem. Mater.*, 11 (1999) 624–633.
- [31] Y.F. Xu, H.T. Hou, Q. Liu, J.Y. Liu, L. Dou, G.R. Qian, Removal behavior research of orthophosphate by CaFe-layered double hydroxides, *Desal. Wat. Treat.*, 57 (2016) 7918–7925.
- [32] J.Z. Zhou, Y.W. Su, J. Zhang, X.X. Xu, J. Zhao, G.R. Qian, Y.F. Xu, Distribution of OH bond to metal-oxide in  $Mg_{3-x}Ca_xFe$ -layered double hydroxide ( $x = 0-1.5$ ): its role in adsorption of selenate and chromate, *Chem. Eng. J.*, 262 (2015) 383–389.
- [33] Y. Lu, H.T. Hou, J. Zhao, J.Z. Zhou, J.Y. Liu, F.F. Lin, G.R. Qian, Enhanced removal of phosphate by hydrocalumite: synergism of  $AlPO_4$  and  $CaHPO_4 \cdot 2H_2O$  precipitation, *Desal. Wat. Treat.*, 57(2016) 7841–7846.

## Supplementary material

Table S1  
List of symbols

Symbols	Annotation of symbols	Unit
[TPP]	The amount of TPP removal	mg/g
[TP] <sub>0</sub>	The initial concentrations of TPP	mg/L
[TP] <sub>e</sub>	The equilibrium concentrations of TPP	mg/L
S	The solid dosing	g/L

Table S2  
The final pH in solution after TPP removal with different samples

Samples	Final pH
Mg <sub>2</sub> Fe-LDO	10.8
Mg <sub>1.5</sub> Ca <sub>0.5</sub> Fe-LDO	10.7
Mg <sub>1.0</sub> Ca <sub>1.0</sub> Fe-LDO	10.5
Mg <sub>0.5</sub> Ca <sub>1.5</sub> Fe-LDO	10.7
Ca <sub>2</sub> Fe-LDO	10.9
Mg <sub>2</sub> Al-LDO	10.1
Mg <sub>1.5</sub> Ca <sub>0.5</sub> Al-LDO	9.9
Mg <sub>1.0</sub> Ca <sub>1.0</sub> Al-LDO	10.2
Mg <sub>0.5</sub> Ca <sub>1.5</sub> Al-LDO	10.7
Ca <sub>2</sub> Al-LDO	10.8